Adsorption of Hexavalent Chromium on KOH Activated Carbon Derived from Water Hyacinth Leaf Coated with Polyaniline/Polypyrrole

Asmamaw Taye*, Solomon Mehretie, Negash Getachew, and Shimelis Admassie

Department of Chemistry, Addis Ababa University, PO Box 1176, Addis Ababa, Ethiopia. E-mail:
asmamaw.taye@aau.edu.et

ABSTRACT: KOH-Activated carbon derived from Water Hyacinth (KOH-WHL-AC) was prepared and coated with Polyaniline-Polypyrrole (PANI/PPY) copolymer for the removal of hexavalent chromium (Cr(VI)) from wastewater. The prepared material was characterized by FT-IR and XRD. The effect of pH, contact time, dosage, and initial Cr(VI) concentrations were optimized using batch adsorption experiment. The adsorption kinetics was found to fit better to pseudo-second-order than the pseudo-first order model. Langmuir and Freundlich isotherm models were analyzed using linear fitting. It was found that the Langmuir adsorption model gives the best fit indicating that the monolayer adsorption of Cr(VI) on the KOH-WHL-AC. The highest adsorption capacity of 409.83 mg/g was achieved at pH 1.0, and equilibrium was achieved within 420 min. The reuse efficiency of the synthesized material was also found to be greater than 54% for five consecutive cycles. Thermodynamic studies have also been carried out and the adsorption was found to be spontaneous and endothermic.

Keywords/Phrases: Activated carbon, Adsorption, Hexavalent chromium, Water hyacinth

INTRODUCTION

Water is valued by all organisms, and it is being polluted by humans due to industrialization and globalization. Fast industrial growth has led to increased elimination and seep of pollutants such as, heavy metals, dyes, pharmaceutical wastes, personal care products, and agricultural wastes into the environment (Narayanasamy et al. 2022). Chromium mainly exists in the trivalent (Cr(III)) and hexavalent (Cr(VI)) oxidation states. Cr(VI) is much more hazardous than Cr(III) due to its higher mobility and toxicity, and referred as a priority pollutant, carcinogen, and mutagenic by world health organization (WHO)(Lu et al. 2021a). Wastewater from mining, dye, paper, electrical appliances, tanneries, paint and electroplating industries are main sources to contaminate the environment with Cr(VI) (Zeng et al. 2021). The permissible level of Cr(VI) is set as 0.5 mg/L in ground water and 0.05 mg/L in drinking water (Ekanayake et al. 2022). Therefore, the removal of Cr(VI) from water systems has become an environmental issue requiring cheap and efficient removal technologies and materials.

The conventional biological treatment processes are not effective in treating chromium wastes due to the nonbiodegradation of Cr(VI) in the environment. Different methods have been developed to deal with heavy metals from aqueous media, including ion exchange (Yang et al. 2014), membrane filtration (Yang et al. 2003), chemical coagulation (Song et al. 2004), electro-dialysis (Peng et al. 2005), redox (Li et al. 2019), and adsorption (Hokkanen et al. 2013). Among these methods, adsorption is the most effective method for removing Cr(VI) from wastewater owing to its low cost, easy availability, less secondary pollution, high selectivity, and high removal efficiency of toxic metals (Enniya et al. 2018; Zhang et al. 2020).

Carbon-based materials (Gu et al. 2013), biomasses (Nameni et al. 2008), metal-organic frameworks (Li et al. 2017), agricultural residues(O'Connell et al. 2008), nanocomposite (Zhang et al. 2018), and polymers (Rafiaee et al. 2020), have been used for the removal of Cr(VI) in wastewater. However, because Cr(VI) is present in wastewater as an oxygen anion, most Cr(VI) adsorbents have a very low adsorption capacity and selectivity. Therefore, the synthesis of materials with high performance and selectivity for Cr(VI) removal has become one of the most pressing problems.

Carbon-based adsorbents are considered to be excellent materials for removing Cr(VI) because of their low cost, highly aromatization, high pore volume, and good adsorption capacity. However,

_____
*Author to whom correspondence should be addressed.

the chemical activation and modification can still increase specific surface area, surface defects, and enhance the adsorption capacity of Cr(VI) (Liang et al. 2021). Some carbon-based adsorbents like, Douglas fir KOH-AC (Herath, Layne, et al. 2021), NaOH-AC produced from agro-industrial waste (Norouzi et al. 2018), Eichhornia crassipes root biomass-derived AC(Giri et al. 2012), Corn stalk-based AC (Zhao et al. 2020), peanut shell AC (AL-Othman et al. 2012), longan seed AC (Yang et al. 2015), Bermuda grass AC (Tu et al. 2020), Mango kernel AC (Rai et al. 2016), chemically modified dried water hyacinth root (Kumar and Chauhan 2019), H_3PO_4 activated and nitrogen-containing modified biochar of Eucalyptus (Lu et al. 2021a), Arundo donax Linn activated carbon amine-crosslinked copolymer (Sun et al. 2013), Palm shell activated carbon with Polyethyleneimine (Owlad et al. 2010), aminated watermelon peel biochar(El-Nemr et al. 2021), nitrogen-doped porous carbon material (Liang et al. 2020), biochar-supported polyaniline hybrid (Herath, Reid, et al. 2021), Polyethyleneimine, and phosphorus codoped hierarchical porous carbons (Chen et al. 2018), were used to remove Cr(VI) from the environment.

Water hyacinth, Brazilian pepper, and some other invasive plant species have been used to remove Cr(VI) from wastewater (Zeng et al. 2021). In particular, the water hyacinth-based adsorbents have an added benefit because they will help to manage this seriously invasive weed and turn it into a useful resource (Sindhu et al. 2017). However, the maximum adsorption capacity of the unmodified water hyacinth products is low. A simple and cost-effective strategy is still required to modify the water hyacinth leaf and enhance the adsorption capacity of Cr(VI). Therefore, in this study, we report for the first time the use of KOH-activated carbon obtained from water hyacinth leaf modified with polyaniline-polypyrrole to enhance the adsorption capacity of Cr(VI).

Abbreviations (AC, Activated Carbon; APS, Ammonium persulfate; Cr(VI), Hexavalent chromium; PZC, Point of zero charge; PANI, Polyaniline; PPY, Polypyrrole; KOH-WHL-AC, Potassium hydroxide Activated Carbon Derived from Water Hyacinth Leaf; WHL, Water hyacinth leaf; WHO, World Health Organization; XRD, Xray diffraction)

MATERIALS AND METHODS

Chemicals and reagents

Chemicals and reagents utilized in this experiment includes; almunium nitrate decahydrate $(Al(NO_3)_3.9H_2O)$, potassium hydroxide (KOH), sodium sulfate (Na_2SO_4, 99%), 1,5-diphenylcarbazide ($C_{13}H_{14}N_4O$ assay, 99%), pyrole (99%), aniline (99.5%) from Sigma Aldrich, Potassium dichromate ($K_2Cr_2O_7$, 99.5%, Carelabmed, India), hydrochloric acid (HCl, 37%, Fluka, Germany), phosphoric acid (H_3PO_4, 98%, Timstar laboratory), sulfuric acid (H_2SO_4, 95-97%, Fluka, Germany), sodium nitrate (NaNO$_3$, 99%, Nice chemicals), sodium hydroxide (NaOH, assay > 97%, RPE, ACS-ISO for analysis), ammonium persulfate ($(NH_4)_2S_2O_8$, assay, 99%, BDH, England), sodium orthophosphate dihydrate ($(Na_2HPO_4).2H_2O$, 99%,Annular analytical reagent, England), sodium chloride (NaCl, 99.5%, Oxford laboratory).

Adsorbent preparation

Water hyacinth leaves (WHL) were collected from Lake Tana, Ethiopia. First, the collected leaf material was cut and washed in tap water until it was clean. Then it was washed with deionized water several times and oven dried at 80^{0}C. The dried WHL was ground to a particle size of roughly 200 µm and washed with 1M HCl.

As the procedure reported within the literature (Shell et al. 2021), 5 g WHL powder was thermally annealed in furnace at 500 ^{0}C under nitrogen for 1 hour. Following thermal annealing, KOH at a 4:1 mass ratio (KOH: biochar) was ground with WHL biochar till it becomes uniform. The mixture was then placed in furnace for activation at 800 ^{0}C under an inert atmosphere for 1 hour. The recovered KOH-WHL-AC was washed using 1M HCl and DI water for several times until it becomes neutral. Finally, it was filtered and dried in a vacuum oven at 80 ^{0}C for 12 hours.

Coating of polypyrrole on KOH-WHL-AC (PPY/KOH-WHL-AC) was done using the procedures reported in reference (Hosseinkhani et al. 2020) with some modifications. Briefly, 20 mL of 1 M HCl was poured into a 250 mL volumetric flask and made up to the mark. Then, 0.1 g of pyrrole and 100 mL of 1 M HCl were added to the first flask. Finally, 0.2 g of synthesized KOH-WHL-AC was added. Along with this, 5 mL of HCl was

poured into a 50 mL volumetric flask, made up to the mark, and added to the second flask. Then, 0.5 g ammonium persulfate (APS) was poured into the second flask and stirred by a magnet for 5 minutes. The first flask containing KOH-WHL-AC, pyrrole, and 1 M HCl was stirred by the magnet and the solution of the second flask containing ammonium persulfate and HCl was dropped through a dropping funnel into the first flask in 30 min. Finally, the synthesized adsorbent was washed three times.

For the synthesis of polyaniline-modified KOH-WHL-AC (PANI/KOH-WHL-AC), KOH-WHL-AC is polymerized with aniline through the following route. In brief, 0.9 g of KOH-WHL-AC was dispersed in 15 mL of 1 M HCl through ultra-sonication for 30 min. To the above dispersion of KOH-WHL-AC, 0.3 mL aniline was added dropwise and again sonicated for 20 min. APS solution (0.912 g APS in 10 mL of water) was added dropwise to the dispersion of aniline and KOH-WHL-AC with continuous stirring for 10 h. A dark green dispersion so developed was filtered through vacuum filtration and washed with HCl and water to eliminate unreacted aniline. The resultant product was oven-dried at 70 ^{0}C for 24 hours(Tripathy et al. 2021).

Polyaniline/Polypyrrole/KOH-WHL-AC (PANI/PPY/KOH-WHL-AC) was prepared as the procedure reported in reference (Dutta et al. 2021). Briefly, 0.1 g of KOH-WHL-AC was dispersed in 10 ml of DI water in a beaker. Similarly, 0.3 ml of pyrrole and 0.15 ml of aniline monomers were mixed individually with 10 ml of DI water in separate beakers and doped with 1 M HCl, and simultaneously added to the dispersion of KOH-WHL-AC by stirring at room temperature for 5 hours. Subsequently, 0.15 g of APS dissolved in DI water was added to the former result and kept in an ice bath for 12 hours. Finally, the obtained product was washed with DI water several times and kept in a vacuum oven at 80 ^{0}C for 24 hours.

Adsorption experiments

The adsorption experiments were conducted in an Erlenmeyer flask with a capacity of 50 mL containing 10 mL of aqueous Cr(VI) solutions of different concentrations and adsorbent dosage of 0.5 g/L of PANI/PPY/KOH-WHL-AC. The solution pH was optimized and maintained at pH

1.0 using 0.1M H_2SO_4, and 0.1M NaOH. The sample flasks were placed in an orbital shaker for agitation at 200 rpm in the time range of 5 to 480 min. Subsequently, the adsorbent was separated by filtering the respective solutions using 0.22 mm Whatman filter paper. Thereafter, the Cr(VI) content in the supernatant liquid was evaluated by using a UV–Vvisible spectrophotometer. The maximum absorbance was measured at 540 nm using 1, 5-diphenyl carbazide in an acidic medium. The adsorption capacity and the % removal of Cr(VI) were calculated using equations (1) and (2) respectively (Dutta et al. 2021).

$$q_e = \frac{(C_o - C_e)V}{m} \qquad (1)$$

$$\% \ Removal = \frac{(C_o - C_e)}{C_0} \times 100 \qquad (2)$$

where q_e represents the equilibrium adsorption capacity, C_o and C_e indicates the initial and equilibrium concentration of Cr(VI) respectively, m (g) is the mass of the adsorbent, and V (L) is the volume of the Cr (VI) solution.

For adsorption kinetic tests, 5 mg of PANI/PPY/KOH-WHL-AC was added to 10 mL Cr(VI) solutions (200 mg/L) at a pH of 1.0 for 5 up to 480 minutes.

Desorption and regeneration experiments

The regeneration studies were conducted at 200 mg/L Cr(VI) concentration, 0.5 g/L adsorbent dosage, the solution pH 1.0, at 25 °C, and shaking for 420 min. The PANI/PPY/KOH-WHL-AC, in the recovered solution, was stirred with excessive 1 M NaOH, for 420 min, and then filtered, washed with distilled water to be neutral, and finally, oven dried at 80 °C for 4 hours. The dried material was taken out and the next adsorption experiment was carried out. The process was repeated six times as supported in reference (Liang et al. 2020).

RESULTS AND DISCUSSION

Characterization of the Adsorbent Materials

The XRD of WHL revealed broad peaks related to intact cellulose at 2θ values of 14° and 22° as shown in Fig. 1. Nevertheless, on carbonizing at 500^{0}C, these peaks were eliminated due to

disruption in cellulose structure. In addition, WHL@500 ⁰C shows numerous new peaks at 2θ 29°, 42°, 51°, and 57° with much intense peak at 29° (see Fig. 1). As supported with reference (Ramirez et al. 2021),CaCO$_3$ and most of the P content was still forming organic structures and that Ca was in the form of CaCO$_3$ which could effectively increase the crystallinity of the biochar that have a remarkable role in Cr(VI) adsorption (Suryawanshi et al. 2023). An increase in disorder of the graphitic sheets of the KOH-WHL-AC enhances the porosity and internal surface area. KOH-WHL-AC shows very weak broad peak at 2θ value of 21° that reflects the efficiency of the preparation process and washing step and proves the competence of KOH as regular activating agents (ElShafei et al. 2017). Moreover, PANI and PPY modified KOH-WHL-AC was highly disordered that enhances the adsorption of Cr(VI).

The WHL, WHL@500 ⁰C, and KOH-WHL-AC underwent FT-IR spectroscopy (see Fig. 2), yielding similar internal molecular results. WHL contained several characteristic peaks including carboxylic acid related O─H bonding peaks at ≈3460, ketone and aldehyde related C═O stretching (1730 cm⁻¹) from the shoulder of the C═C (aromatic/straight chain) peak located at ≈1635 cm⁻¹. The bonds in WHL are characteristics of lignocelluloses in which cyclic and aromatic compounds are frequently bonded to functional groups of O─H, COOH, R─C─O─C─R, and C═O for lignin, hemicelluloses, and cellulose. After thermal carbonization at 500 ⁰C, FTIR spectra patterns change significantly. Most of the O─H compounds including bonded alcohols and carboxylic acids have been gasified and removed from the solid product. The pronounced peaks corresponding to S═O ≈ 1400 cm⁻¹ were disappeared and the peak correlating with an increase in aromatic C═C stretching is observed at ≈1560 cm⁻¹. The KOH-WHL-AC resulting from the high temperature thermo-chemical and catalytic activation of WHL@500 ⁰C demonstrated cleavage of all functional groups leaving a primarily carbon structure. A weak peak at ≈ 1635 cm⁻¹ indicates C═C stretching involving aromatics alkenes(Shell et al. 2021).The bands at ≈ 3450 cm⁻¹ and 1650 cm⁻¹areobserved for PANI/KOH-WHL-AC which are attributed to the N–H stretching of aromatic amine and C=N stretching vibration of the quinoid ring respectively. The broad and shallow band peak at ≈ 3460 cm⁻¹ and the small peak at ≈ 2900 cm⁻¹ exhibits the presence of an amine functional group and sp³ C-H stretching of PANI/PPY/KOH-WHL-AC, respectively. Minor shifting of band wavelengths and the decrease in intensity of peak for PANI/PPY/KOH-WHL-AC-Cr(VI) could be attributed to the steric hindrance of Cr(VI) complex with the adsorbent material (Alemayehu Yifru et al. 2022).
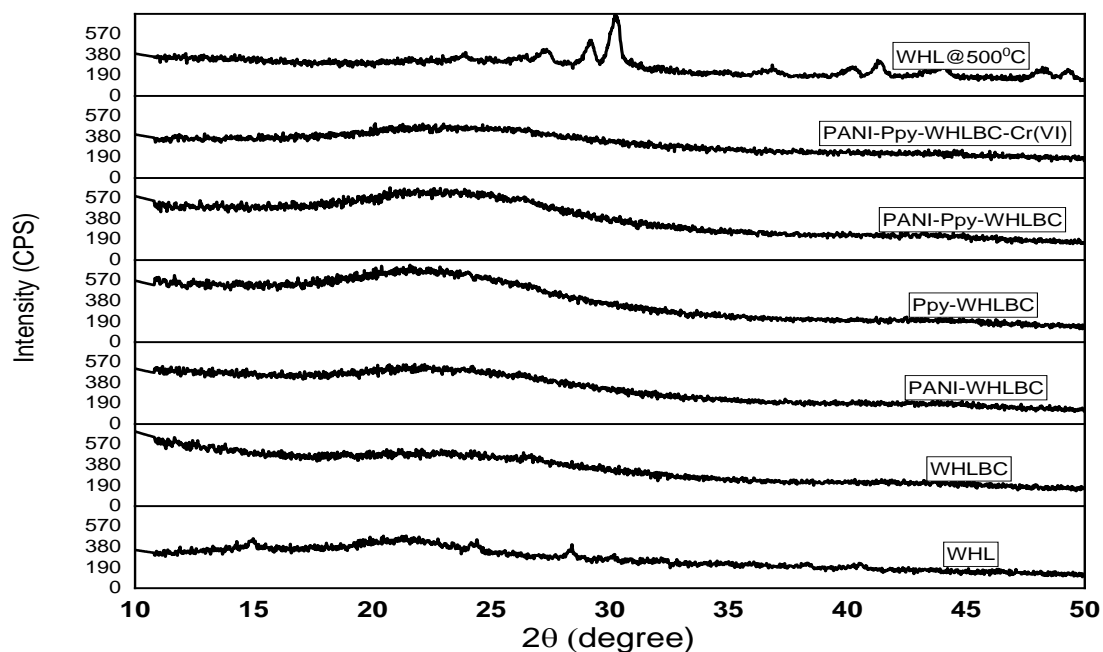
Figure 1. XRD patterns of WHL, KOH-WHL-AC, PANI/KOH-WHL-AC, PPY/KOH-WHL-AC, PANI/PPY/KOH-WHL-AC, PANI/PPY/KOH-WHL-AC-Cr(VI), and WHL@50 0⁰C.
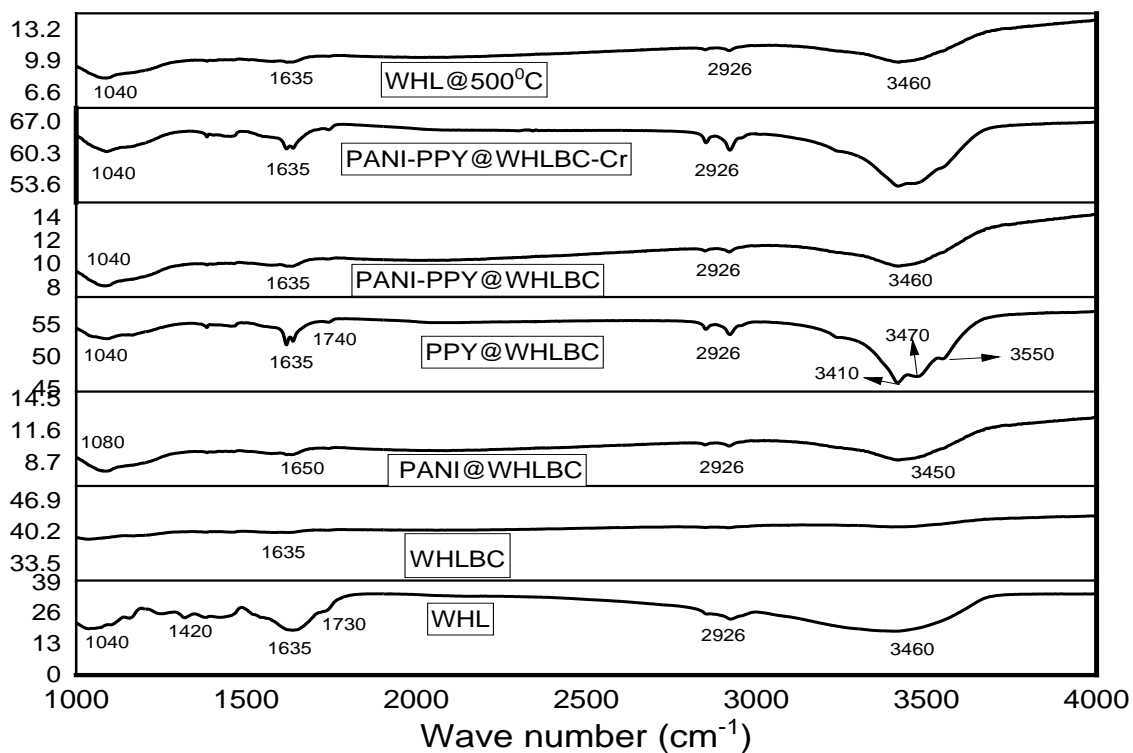

Figure 2. FT-IR spectra of WHL, KOH-WHL-AC, PANI/KOH-WHL-AC, PPY/KOH-WHL-AC, PANI-PPY@KOH-WHL-AC, PANI-PPY@KOH-WHL-AC-Cr(VI), and WHL@500 ⁰C.

Effect of solution pH, adsorbent dosage, contact time, and kinetics on the adsorption of Cr(VI)

The effect of pH on the adsorption of Cr(VI) by PANI/PPY/KOH-WHL-AC was studied at different pH values of (1.0-7.0) as shown in Fig. 3a. The optimum pH of solution was observed at pH of 1.0 with increasing pH resulting in a drastic decrease in adsorption capacity. Cr(VI) mainly exists as H_2CrO_4 at pH < 1.0, $HCrO_4^-$ and $Cr_2O_7^{2-}$ at pH (2.0 – 6.0) (Tripathy et al. 2021).The pH of point of zero charge (PZC) of surface of PANI-PPY/KOH-WHL-AC was found to be 3.6. When the pH is less than PZC, the amine groups on surface of PANI/PPY/KOH-WHL-AC are protonated, the adsorbent becomes positively charged which is suitable for electrostatic attraction between the adsorbent and Cr(VI) oxyanions. When the pH is 1.0, the surface of PANI-PPY/KOH-WHL-AC presents a maximum protonation and maximum adsorption capacity is obtained. In contrast, the surface of PANI-PPY/KOH-WHL-AC is deprotonated, resulting in a negative surface charge and hindering the adsorption process of Cr(VI) (Lu et al. 2021a).

The effect of adsorbent dosage experiments was carried out at initial concentration of Cr(VI) 200 mg/L, pH 1.0, contact time 420 min and temperature of 298 K as shown in Fig 3c. The removal rate was increased from 87.12% at 0.5 g/L to 100% at 1.5 g/L, and the adsorption capacity was decreased from 348.23 to 133.57 mg/g. This can be attributed to the increase in adsorbent mass and surface area increased the number of active adsorption sites. Hence, the amount of Cr(VI) adsorbed per unit mass of adsorbent decreases with increasing adsorbent mass, resulting in reduction in both effective surface area and adsorbate/adsorbent ratio (Zhang et al. 2010).

The effect of contact time between the adsorbent and Cr(VI) solution on adsorption capacity was shown in Fig. 3c. Adsorption increases with increasing contact time because a large number of active and vacant sites will be occupied over the time. Therefore, this increasing trend in adsorption will be more significant at the beginning and will decline later and causes a slight increase in adsorption capacity (Rafiaee et al. 2020). In this study the adsorption capacity abruptly increased up to 150 min, then steadily increases up to 420 min and remains constant after 420 min. Hence the optimum contact time 420 min is chosen for further experiments. In order to analyze the kinetic behavior of Cr(VI) on the adsorbent PANI-PPY@ KOH-WHL-AC, both the pseudo-first-order and the pseudo-second-order kinetic model was used (Rai et al. 2016). The pseudo-first-order and pseudo-second-order equations (3) and (4) are used for kinetic studies.

$$ln\ (q_e - q_t) = ln\ q_e - k_1 t \qquad (3)$$

$$\frac{t}{q_t} = \frac{1}{k_2 q_e^2} + \frac{t}{q_e} \qquad (4)$$

where q_t (mg/g) is the amount of adsorbate adsorbed at time t (min), q_e (mg/g) is the equilibrium adsorption capacity, k_1 and k_2 are the rate constants of pseudo-first-order and pseudo-second-order kinetic models respectively.

Close agreement between experimental and calculated kinetic constants and coefficient of correlation was observed, indicating that the pseudo second order model better represents the experimental data. It reveals that chemical adsorption is more favourable than physical process as shown in Fig 4d.
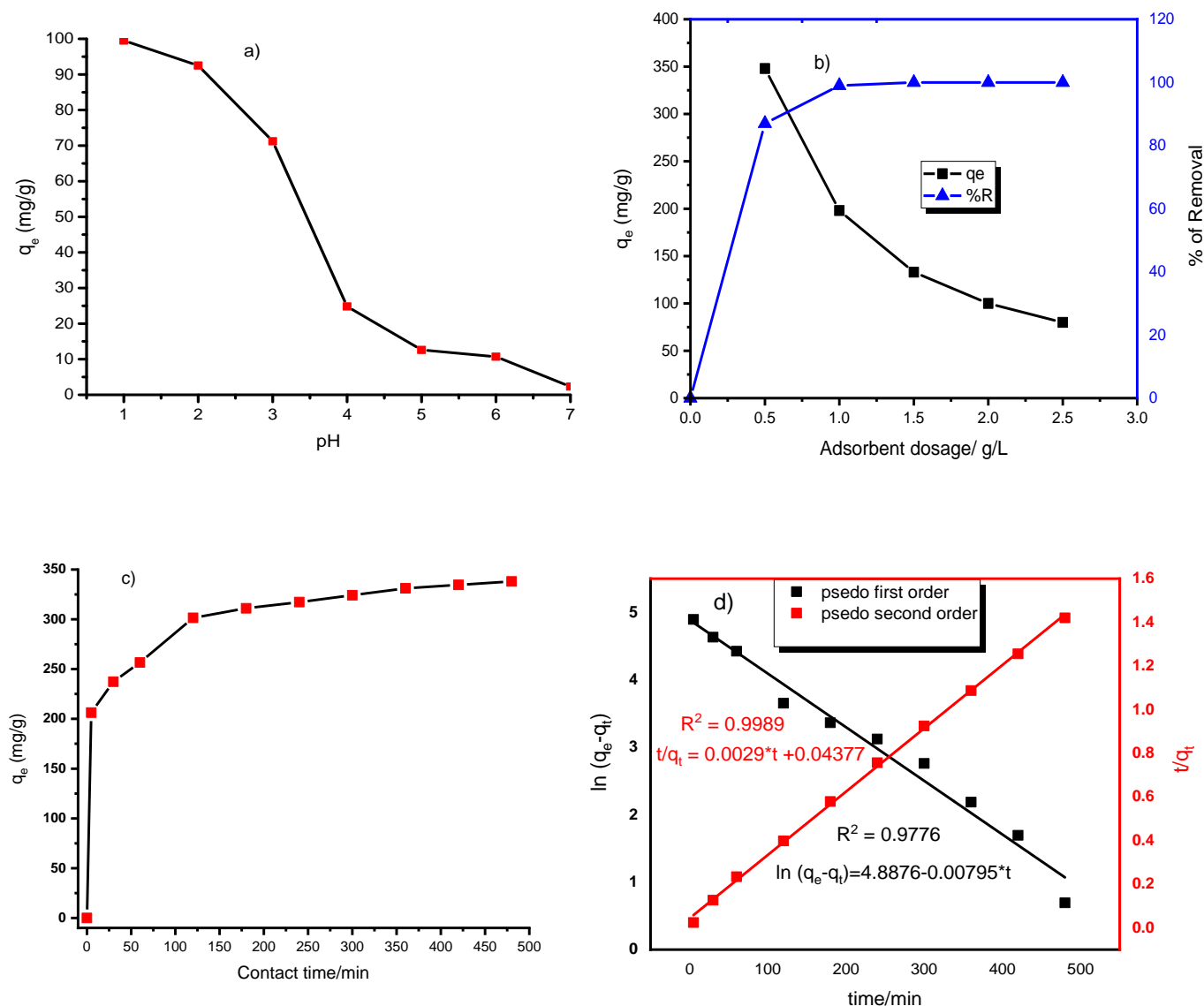
Figure 3. The effect of: a) pH (contact time 1hour; [Cr(VI)]$_0$, 100 mg/L; adsorbent dosage 1 g/L), b) adsorbent dosage (pH 1.0; contact time 420 min; [Cr(VI)]$_0$, 200 mg/L), c) contact time (pH , 1.0, adsorbent dosage 0.5 g/L, [Cr(VI)]$_0$, 200 mg/L) using PANI-PPY/KOH-WHL-AC, and d) pseudo first-order and pseudo second-order kinetic model fitting.

The effect of equilibrium concentration, adsorption equilibrium and thermodynamics studies

Equilibrium studies were carried by shaking Cr(VI) solutions of different concentrations (50–350 mg/L) with 0.5 g/L PANI-PPY?KOH-WHL-AC for 420 min at pH value of 1.0. The effect of the equilibrium concentration of Cr(VI) on adsorbents of WHL, WHL@500 ^{0}C, KOH-WHL-AC, PANI/KOH-WHL-AC, PPY/KOH-WHL-AC, and PANI/PPY/KOH-WHL-AC was studied at the optimized conditions as shown in Fig. 4a. In the

beginning, the Cr(VI) uptake increased with increasing equilibrium Cr(VI) concentration and that gradually reduced at higher concentrations and eventually became constant for all the used adsorbents. After a certain level of increase in equilibrium Cr(VI) concentration, all the active sites on the adsorbent surface get occupied and finally establish a form of dynamic equilibrium between the processes of adsorption and desorption (Rai et al. 2016).The experimental data were then analyzed by linear fitting into the

Langmuir and Freundlich isotherms (see Fig. 4 a, b and Table 1) using equations (5) and (6) respectively (Subramanyam and Das 2014).

$$\frac{1}{q_e} = \frac{1}{K_L q_m} \, x \, \frac{1}{C_e} + \frac{1}{q_m} \tag{5}$$

$$\ln(q_e) = \ln(K_F) + \frac{1}{n} \ln(Ce) \tag{6}$$

where q_e (mg/g) is the equilibrium adsorption capacity, Ce (mg/L) is the equilibrium concentration, K_L (L/mg) is the Langmuir adsorption constant, q_m (mg/g) is the maximum adsorption capacity, K_F is the Freundlich constant, $1/n$ is the heterogeneity factor.

The isotherm model fitting reveals that, the Langmuir adsorption model best fit with the adsorption process because it has linear correlation coefficient ($R^2 = 0.9997$) as oppose to Freundlich model ($R^2 = 0.8437$). The calculated adsorption coefficient q_m was found to be 409.84 mg/g which was closer to the actual adsorption data of 404.85 mg/g. The result indicates that single layer removal was observed at the surface of the adsorbent.

Table 1. The parameters of the adsorption isotherms for Cr(VI) removal by PANI/PPY/KOH-WHL-AC.

Langmuir isotherm model			Freundlich isotherm model		
q_m (mg/g)	K_L (L/mg)	R^2	n	K_f	R^2
409.84	0.39	0.9997	4.35	150.05	0.8437

The effect of temperature on the adsorption of Cr (VI) was investigated at optimized conditions. The adsorption capacity of Cr(VI) increased from 318.7-397.31 mg/g for the temperature range of 298–318 K. The increase in adsorption capacity with the increase in temperature indicates that the adsorption process is endothermic in nature and heat can promote the combination of active sites with Cr(VI) (Giri et al. 2012).

The thermodynamic parameters for the adsorption process were calculated by using equations (7), (8) and (9) (Lu et al. 2021b).

$$G = -RT \ln Kc \tag{7}$$

$$Kc = \frac{C_A}{C_S} \tag{8}$$

$$\ln Kc = \frac{-\Delta H}{RT} + \frac{\Delta S}{R} \tag{9}$$

where R (8.314 J mol^{-1} k^{-1}) is the gas constant, Kc is the equilibrium constant, T (K) is the temperature, C_A and C_S (mg/L) are the equilibrium concentrations of Cr(VI) on the adsorbent and in the solution, respectively, ΔH is standard enthalpy, and ΔS is the entropy of the adsorption system.

Linear fitting of ln Kc vs 1/T is illustrated in Fig. 4d and specific parameters were given in Table 3. The positive ΔS values suggest the degree of freedom at the solid-liquid interface decreased during the adsorption process. This reflects the accidental decrease in the solid-liquid interface and the reduced affinity of Cr(VI) for the adsorbent. The negative value of ΔG at various temperatures proposed that Cr(VI) adsorption process was spontaneous and thermodynamically favorable. When the temperature increased from 298 K - 318 K, the values of ΔG decreased from -3.39 to -7.19 kJ/mol. The smaller value of ΔG highly favors the adsorption process, which indicates the rise in temperature is consequently beneficial to the adsorption process (Lu et al. 2021a).
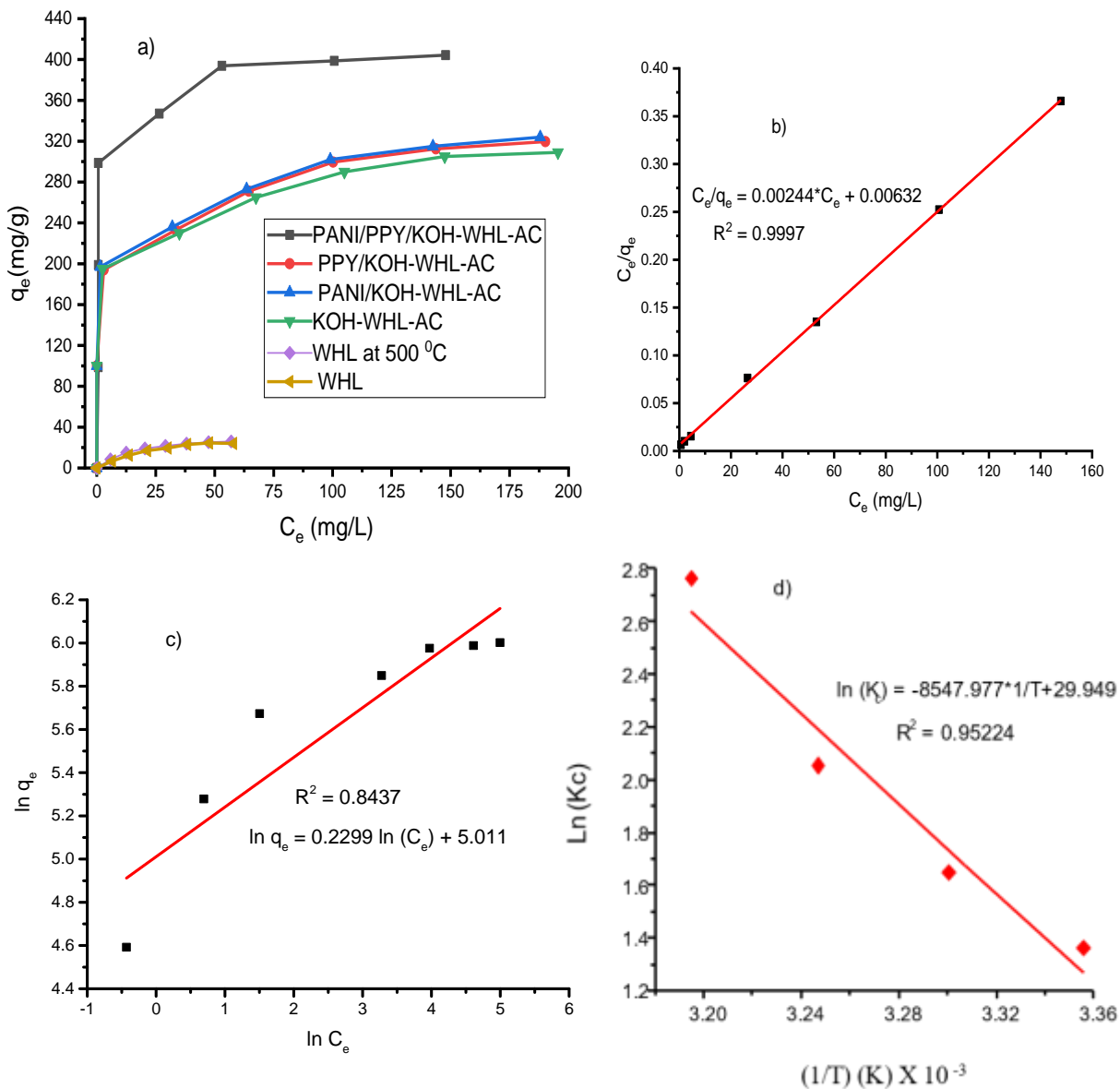
Figure 4. a) effect equilibrium concentration, b) linear fitting of Langmuir model, c) linear fitting of Freundlich model, and d) thermodynamic parameters on the adsorption capacity of Cr(VI) (Conditions, pH 1.0; [Cr(VI)]$_0$, 200 mg/L; adsorbent dosage 0.5 g/L).

The effect of interference

In wastewater containing Cr(VI), there are many competing ions. Therefore, in the solution containing 200 mg/L of Cr(VI) solutions, (100, 300 and 600) mg/L of other ions (SO_4^{2-}, HPO_4^-, HCO_3^-, Cl^- and NO_3^-) were added to explore the selective adsorption of Cr(VI) on PANI/PPY/KOH-WHL-AC. The result indicated that PANI/PPY/KOH-WHL-AC had an excellent selectivity on Cr(VI) adsorption. For all the selected competing anions, as the concentration of the interferences increases, the removal efficiency and the adsorption capacity of Cr(VI) decreases slightly.
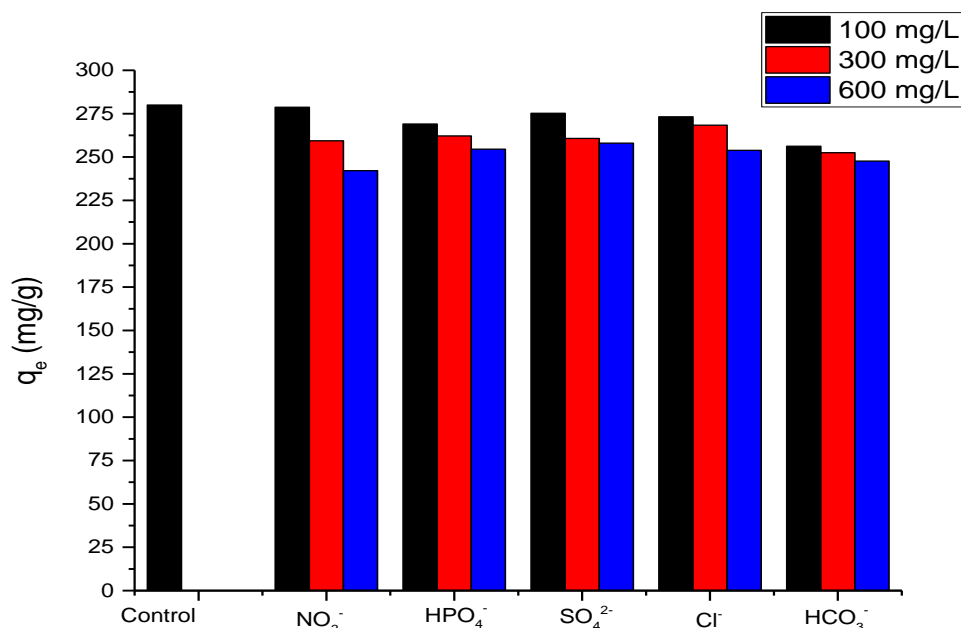
Figure 5. The effect of interference on the adsorption capacity of Cr (VI).

Reusability study

The reusability of PANI-PPY/KOH-WHL-AC determines its applicability in wastewater treatment. Therefore, desorption was done by transferring 50 mg of PANI-PPY/KOH-WHL-AC saturated with 200 mg/L Cr(VI) solutions to flasks containing excess amount of1 M NaOH. The reuse efficiency of PANI/PPY/KOH-WHL-AC decreases up to 55.40 % in the first five desorption recycling experiments as shown in Fig. 6. It can be generalized that PANI-PPY/KOH-WHL-AC is suitable for the re-adsorption of heavy metals from wastewater (Tripathy et al. 2021).
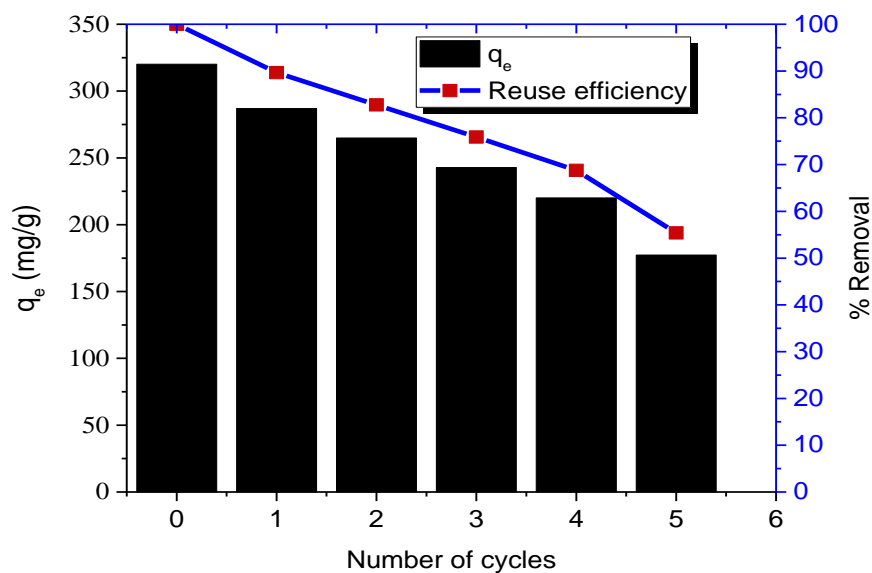

Figure 6. PANI/PPY/KOH-WHL-AC recycling study (pH 1.0; contact time 420 min; initial concentration of Cr (VI) = 200 mg/L).

The maximum adsorption capacities of different adsorbents for the removal of Cr(VI) were compared with similar adsorbent materials reported in the literatures as depicted in Table 2.

Table 2. Comparison of Cr(VI) adsorption capacity of different adsorbents.

Types of adsorbents	q_m(mg/ g)	References
KOH-activated Douglas fir biochar	127.2	(Herath, Layne, et al. 2021)
NaOH-activated carbon produced from agro-industrial waste	282.8	(Norouzi et al. 2018)
Eichhornia crassipes root biomass-derived activated carbon	36.3	(Giri et al. 2012)
Corn stalk-based activated carbon	89.5	(Zhao et al. 2020)
Activated carbon prepared from peanut shell	16.3	(AL-Othman et al. 2012)
Activated carbon prepared from longan seed	169.5	(Yang et al. 2015)
Activated carbon derived from Bermuda grass	403.2	(Tu et al. 2020)
H_3PO_4 activated carbon prepared from mango kernel	7.8	(Rai et al. 2016)
Chemically modified dried water hyacinth root	1.3	(Kumar and Chauhan 2019)
H_3PO_4 activated and nitrogen-containing modified biochar of Eucalyptus	250.0	(Lu et al. 2021a)
Arundo donax Linn activated carbon amine-crosslinked copolymer	102.9	(Sun et al. 2013)
Palm shell activated carbon with Polyethyleneimine	228.2	(Owlad et al. 2010)
Aminated watermelon peel biochar	333.3	(El-Nemr et al. 2021)
Nitrogen-doped porous carbon material	402.9	(Liang et al. 2020)
Biochar-supported polyaniline hybrid	150.0	(Herath, Reid, et al. 2021)
Polyethylenimine and phosphorus codoped hierarchical porous carbons	355.0	(Chen et al. 2018)
PANI/PPY/KOH-WHL-AC	409.83	This work

The adsorption capacity of PANI-PPY@KOH-WHL-AC was higher than all the listed activated and modified carbon adsorbents, indicating that the prepared material enhanced the adsorption capacity. Accordingly, PANI-PPY@KOH-WHL-AC is a promising and even the best of all water hyacinth-based adsorbents reported for the removal of Cr(VI) from aqueous solutions.

CONCLUSION

PANI/PPY/KOH-WHL-AC was successfully prepared for the removal of Cr(VI) ions in wastewater. The best Cr(VI) uptake conditions were, solution pH value of 1.0, initial Cr(VI) concentration of 200 mg/L, and adsorbent dosage of 0.5 g/L. Kinetic and isotherm studies revealed that chemisorption was the most likely predominant mechanism with a maximum adsorption capacity of 409.85 mg/g. The adsorbent had excellent removal performance, scalable, cheap, and can be used for five different consecutive cycles efficiently for the removal of Cr(VI). These findings highlighted the value of an invasive water hyacinth weed and it is an excellent opportunity to convert 'trash in to treasure'. It is a green, economical, and high-performance adsorbent for applications in heavy metal wastewater treatment.

REFERENCES

1. AL-Othman ZA, Ali R, Naushad Mu. 2012. Hexavalent chromium removal from aqueous medium by activated carbon prepared from peanut shell: Adsorption kinetics, equilibrium and thermodynamic studies. *Chemical Engineering Journal.* 184:238–247. doi:10.1016/j.cej.2012.01.048.

2. Chen S, Wang J, Wu Z, Deng Q, Tu W, Dai G, Zeng Z, Deng S. 2018. Enhanced Cr(VI) removal by polyethylenimine- and phosphorus-codoped hierarchical porous carbons. *Journal of Colloid and Interface Science.* 523:110–120. doi: 10.1016/j.jcis.2018.03.057.

3. Dutta S, Srivastava SK, Gupta AK. 2021. Polypyrrole–polyaniline copolymer coated green rice husk ash as an effective adsorbent for the removal of hexavalent chromium from contaminated

water. *Mater Adv.* 2(7):2431–2443. doi:10.1039/D0MA00862A.

4. Ekanayake A, Rajapaksha AU, Selvasembian R, Vithanage M. 2022. Amino-functionalized biochars for the detoxification and removal of hexavalent chromium in aqueous media. *Environmental Research.* 211:113073. doi:10.1016/j.envres.2022.113073.

5. El-Nemr MA, Ismail IMA, Abdelmonem NM, El Nemr A, Ragab S. 2021. Amination of biochar surface from watermelon peel for toxic chromium removal enhancement. *Chinese Journal of Chemical Engineering.* 36:199–222. doi:10.1016/j.cjche.2020.08.020.

6. ElShafei GMS, ElSherbiny IMA, Darwish AS, Philip CA. 2017. Artichoke as a non-conventional precursor for activated carbon: Role of the activation process. *Journal of Taibah University for Science.* 11(5):677–688. doi:10.1016/j.jtusci.2016.04.006.

7. Enniya I, Rghioui L, Jourani A. 2018. Adsorption of hexavalent chromium in aqueous solution on activated carbon prepared from apple peels. *Sustainable Chemistry and Pharmacy.* 7:9–16. doi:10.1016/j.scp.2017.11.003.

8. Giri AK, Patel R, Mandal S. 2012. Removal of Cr (VI) from aqueous solution by Eichhornia crassipes root biomass-derived activated carbon. *Chemical Engineering Journal.* 185–186:71–81. doi:10.1016/j.cej.2012.01.025.

9. Gu H, Rapole SB, Huang Y, Cao D, Luo Z, Wei S, Guo Z. 2013. Synergistic interactions between multi-walled carbon nanotubes and toxic hexavalent chromium. *J Mater Chem* A. 1(6):2011–2021. doi:10.1039/C2TA00550F.

10. Herath A, Layne CA, Perez F, Hassan EB, Pittman CU, Mlsna TE. 2021. KOH-activated high surface area Douglas Fir biochar for adsorbing aqueous Cr(VI), Pb(II) and Cd(II). *Chemosphere.* 269:128409. doi:10.1016/j.chemosphere.2020.128409.

11. Herath A, Reid C, Perez F, Pittman CU, Mlsna TE. 2021. Biochar-supported polyaniline hybrid for aqueous chromium and nitrate adsorption. J*ournal of Environmental Management.* 296:113186. doi:10.1016/j.jenvman.2021.113186.

12. Hokkanen S, Repo E, Sillanpää M. 2013. Removal of heavy metals from aqueous solutions by succinic anhydride modified mercerized nanocellulose. *Chemical Engineering Journal.* 223:40–47. doi:10.1016/j.cej.2013.02.054.

13. Hosseinkhani A, Forouzesh Rad B, Baghdadi M. 2020. Efficient removal of hexavalent chromium from electroplating wastewater using polypyrrole coated on cellulose sulfate fibers.

Journal of Environmental Management. 274:111153. doi:10.1016/j.jenvman.2020.111153.

14. Kumar P, Chauhan MS. 2019. Adsorption of chromium (VI) from the synthetic aqueous solution using chemically modified dried water hyacinth roots. *Journal of Environmental Chemical Engineering.* 7(4):103218. doi:10.1016/j.jece.2019.103218.

15. Li L-L, Feng X-Q, Han R-P, Zang S-Q, Yang G. 2017. Cr(VI) removal via anion exchange on a silver-triazolate MOF. *Journal of Hazardous Materials.* 321:622–628. doi:10.1016/j.jhazmat.2016.09.029.

16. Li M-Y, Guo W-Q, Guo G-L, Zhu X-M, Niu X-T, Shan X-F, Tian J-X, Wang G-Q, Zhang D-M. 2019. Effect of sub-chronic exposure to selenium and Allium mongolicum Regel flavonoids on Channa argus: Bioaccumulation, oxidative stress, immune responses and immune-related signaling molecules. *Fish & Shellfish Immunology.* 91:122–129. doi:10.1016/j.fsi.2019.05.002.

17. Liang H, Sun R, Song B, Sun Q, Peng P, She D. 2020. Preparation of nitrogen-doped porous carbon material by a hydrothermal-activation two-step method and its high-efficiency adsorption of Cr(VI). *Journal of Hazardous Materials.* 387:121987. doi:10.1016/j.jhazmat.2019.121987.

18. Liang H, Zhang H, Zhao P, Zhao X, Sun H, Geng Z, She D. 2021. Synthesis of a novel three-dimensional porous carbon material and its highly selective Cr(VI) removal in wastewater. *Journal of Cleaner Production.* 306:127204. doi:10.1016/j.jclepro.2021.127204.

19. Lu Z, Zhang H, Shahab A, Zhang K, Zeng H, Bacha A-U-R, Nabi I, Ullah H. 2021a. Comparative study on characterization and adsorption properties of phosphoric acid activated biochar and nitrogen-containing modified biochar employing Eucalyptus as a precursor. *Journal of Cleaner Production.* 303:127046. doi:10.1016/j.jclepro.2021.127046.

20. Lu Z, Zhang H, Shahab A, Zhang K, Zeng H, Bacha A-U-R, Nabi I, Ullah H. 2021b. Comparative study on characterization and adsorption properties of phosphoric acid activated biochar and nitrogen-containing modified biochar employing Eucalyptus as a precursor. *Journal of Cleaner Production.* 303:127046. doi:10.1016/j.jclepro.2021.127046.

21. Nameni M, Alavi Moghadam MR, Arami M. 2008. Adsorption of hexavalent chromium from aqueous solutions by wheat bran. *Int J Environ Sci Technol.* 5(2):161–168. doi:10.1007/BF03326009.

22. Narayanasamy S, Sundaram V, Sundaram T, Vo D-VN. 2022. Biosorptive ascendency of plant

based biosorbents in removing hexavalent chromium from aqueous solutions – Insights into isotherm and kinetic studies. *Environmental Research.* 210:112902. doi:10.1016/j.envres.2022.112902.

23. Norouzi S, Heidari M, Alipour V, Rahmanian O, Fazlzadeh M, Mohammadi-moghadam F, Nourmoradi H, Goudarzi B, Dindarloo K. 2018. Preparation, characterization and Cr(VI) adsorption evaluation of NaOH-activated carbon produced from Date Press Cake; an agro-industrial waste. *Bioresource Technology.* 258:48–56. doi:10.1016/j.biortech.2018.02.106.

24. O'Connell DW, Birkinshaw C, O'Dwyer TF. 2008. Heavy metal adsorbents prepared from the modification of cellulose: A review. *Bioresource Technology.* 99(15):6709–6724. doi:10.1016/j.biortech.2008.01.036.

25. Owlad M, Aroua MK, Wan Daud WMA. 2010. Hexavalent chromium adsorption on impregnated palm shell activated carbon with polyethyleneimine. *Bioresource Technology.* 101(14):5098–5103. doi:10.1016/j.biortech.2010.01.135.

26. Peng C, Meng H, Song S, Lu S, Lopez-Valdivieso A. 2005. Elimination of Cr(VI) from Electroplating Wastewater by Electrodialysis Following Chemical Precipitation. *Separation Science and Technology.* 39(7):1501–1517. doi:10.1081/SS-120030788.

27. Rafiaee S, Samani MR, Toghraie D. 2020. Removal of hexavalent chromium from aqueous media using pomegranate peels modified by polymeric coatings: Effects of various composite synthesis parameters. *Synthetic Metals.* 265:116416. doi:10.1016/j.synthmet.2020.116416.

28. Rai MK, Shahi G, Meena V, Meena R, Chakraborty S, Singh RS, Rai BN. 2016. Removal of hexavalent chromium Cr (VI) using activated carbon prepared from mango kernel activated with H3PO4. *Resource-Efficient Technologies.* 2:S63–S70. doi:10.1016/j.reffit.2016.11.011.

29. Ramirez A, Pérez S, Flórez E, Acelas N. 2021. Utilization of water hyacinth (Eichhornia crassipes) rejects as phosphate-rich fertilizer. *Journal of Environmental Chemical Engineering.* 9(1):104776. doi:10.1016/j.jece.2020.104776.

30. Shell KM, Vohra SY, Rodene DD, Gupta RB. 2021. Phytoremediation of Nickel via Water Hyacinth for Biocarbon-Derived Supercapacitor Applications. *Energy Technol.* 9(8):2100130. doi:10.1002/ente.202100130.

31. Sindhu R, Binod P, Pandey A, Madhavan A, Alphonsa JA, Vivek N, Gnansounou E, Castro E, Faraco V. 2017. Water hyacinth a potential source for value addition: An overview. *Bioresource Technology.* 230:152–162. doi:10.1016/j.biortech.2017.01.035.

32. Song Z, Williams CJ, Edyvean RGJ. 2004. Treatment of tannery wastewater by chemical coagulation. *Desalination.* 164(3):249–259. doi:10.1016/S0011-9164(04)00193-6.

33. Subramanyam B, Das A. 2014. Linearised and non-linearised isotherm models optimization analysis by error functions and statistical means. *J Environ Health Sci Engineer.* 12(1):92. doi:10.1186/2052-336X-12-92.

34. Sun Y, Yue Q, Gao B, Gao Y, Li Q, Wang Y. 2013. Adsorption of hexavalent chromium on Arundo donax Linn activated carbon amine-crosslinked copolymer. *Chemical Engineering Journal.* 217:240–247. doi:10.1016/j.cej.2012.11.121.

35. Suryawanshi SS, Kamble PP, Gurav R, Yang Y-H, Jadhav JP. 2023. Statistical comparison of various agricultural and non-agricultural waste biomass-derived biochar for methylene blue dye sorption. *Biomass Conv Bioref.* 13(6):5353–5366. doi:10.1007/s13399-021-01636-1.

36. Tripathy S, Sahu S, Patel RK, Panda RB, Kar PK. 2021. Efficient removal of Cr(VI) by polyaniline modified biochar from date (Phoenix dactylifera) seed. *Groundwater for Sustainable Development.* 15:100653. doi:10.1016/j.gsd.2021.100653.

37. Tu B, Wen R, Wang K, Cheng Y, Deng Y, Cao W, Zhang K, Tao H. 2020. Efficient removal of aqueous hexavalent chromium by activated carbon derived from Bermuda grass. *Journal of Colloid and Interface Science.* 560:649–658. doi:10.1016/j.jcis.2019.10.103.

38. Yang J, Yu M, Chen W. 2015. Adsorption of hexavalent chromium from aqueous solution by activated carbon prepared from longan seed: Kinetics, equilibrium and thermodynamics. *Journal of Industrial and Engineering Chemistry.* 21:414–422. doi:10.1016/j.jiec.2014.02.054.

39. Yang J, Yu M, Qiu T. 2014. Adsorption thermodynamics and kinetics of Cr(VI) on KIP210 resin. *Journal of Industrial and Engineering Chemistry.* 20(2):480–486. doi:10.1016/j.jiec.2013.05.005.

40. Yang W-P, Zhang Z-J, Deng W. 2003. Simultaneous, sensitive and selective on-line chemiluminescence determination of Cr(III) and Cr(VI) by capillary electrophoresis. *Analytica Chimica Acta.* 485(2):169–177. doi:10.1016/S0003-2670(03)00421-5.

41. Yifru A, Mekonnen N, Mehretie S, Admassie S. 2022. Polypyrrole–polyaniline-water hyacinth leaf protein concentrate composite for the

removal of Cr(VI) from aqueous solution: kinetics, isotherm and thermodynamic studies. *Bull Chem Soc Eth*. 36(3):571–584. doi:10.4314/bcse.v36i3.7.

42. Zeng Huiting, Zeng Honghu, Zhang H, Shahab A, Zhang K, Lu Y, Nabi I, Naseem F, Ullah H. 2021. Efficient adsorption of Cr (VI) from aqueous environments by phosphoric acid activated eucalyptus biochar. *Journal of Cleaner Production*. 286:124964. doi:10.1016/j.jclepro.2020.124964.

43. Zhang H, Tang Y, Cai D, Liu X, Wang X, Huang Q, Yu Z. 2010. Hexavalent chromium removal from aqueous solution by algal bloom residue derived activated carbon: Equilibrium and kinetic studies. *Journal of Hazardous Materials*. 181(1–3):801–808. doi:10.1016/j.jhazmat.2010.05.084.

44. Zhang Q, Dong K, Liu Qiang, Liu Qinze, Yao J. 2020. Green and simple synthesis of poly (catechol-tetraethylenepentamine)@aminopropyl-modified silica composite for removing toxic Cr(VI). *Journal of the Taiwan Institute of Chemical Engineers*. 110:112–119. doi:10.1016/j.jtice.2020.03.002.

45. Zhang S-H, Wu M-F, Tang T-T, Xing Q-J, Peng C-Q, Li F, Liu H, Luo X-B, Zou J-P, Min X-B, et al. 2018. Mechanism investigation of anoxic Cr(VI) removal by nano zero-valent iron based on XPS analysis in time scale. *Chemical Engineering Journal*. 335:945–953. doi:10.1016/j.cej.2017.10.182.

46. Zhao J, Yu L, Ma H, Zhou F, Yang K, Wu G. 2020. Corn stalk-based activated carbon synthesized by a novel activation method for high-performance adsorption of hexavalent chromium in aqueous solutions. *Journal of Colloid and Interface Science*. 578:650–659. doi:10.1016/j.jcis.2020.06.031.